

Synthesis of aminoalkylsilanes with oligo(ethylene oxide) unit as multifunctional electrolyte additives for lithium-ion batteries

WANG JingLun, LUO Hao, MAI YongJin, ZHAO XinYue & ZHANG LingZhi*

Guangzhou Institute of Energy Conversion, Chinese Academy of Sciences, Guangzhou 510640, China

Received October 29, 2012; accepted January 14, 2013; published online April 11, 2013

Aminoalkylsilanes with oligo(ethylene oxide) units were designed and synthesized as multifunctional electrolyte additives for lithium-ion batteries. The chemical structures were fully characterized by nuclear magnetic resonance (NMR) spectroscopy and their thermal properties, viscosities, electrochemical windows, and ionic conductivities were systematically measured. With adding one of these compounds (1 vol. %, DSC3N1) in the baseline electrolyte 1.0 M LiPF₆ in EC:DEC (1:1, in volume), Li/LiCoO₂ half cell tests showed an improved cyclability after 100 cycles and improved rate capability at 5C rate condition. Electrochemical impedance spectroscopy (EIS), X-ray photoelectron spectroscopy (XPS), and energy dispersive spectroscopic (EDS) analysis confirmed the acid scavenging function and film forming capability of DSC3N1. These results demonstrated that the multifunctional organosilicon compounds have considerable potential as additives for use in lithium-ion batteries.

aminoalkylsilane, electrolyte additives, lithium cobalt oxide, lithium-ion batteries

1 Introduction

Recently, much effort has been devoted to developing advanced electrolyte materials to satisfy the ever-increasing applications of lithium-ion batteries (LIBs) demanding high energy density and safety [1]. The development of functional electrolyte additives is recognized as one of the most economic and effective methods to improve the performance of LIBs [2]. Various kinds of additives have been reported so far, including film forming additives [3], flame retardant additives [4], high/low temperature additives [5], over charge additives [6], and high voltage additives [7].

Organosilicon compounds have received much attention as electrolytes for energy storage devices due to their thermal and electrochemical stability, less flammable and environmentally benign characteristics [8]. West and Amine *et al.* systematically studied the synthesis and electrochemical properties of organosilicon compounds functionalized with

oligo(ethylene oxide) substituents as electrolyte solvents for LIBs [9]. On the other hand, it has also been reported that the electrochemical performances of LIBs could be improved remarkably by adding a small amount of organosilicon additives in the conventional alkylcarbonate based electrolytes [10]. Takechi and Shiga disclosed a series of “Si–N” based additives, such as *N,N*-diethylamino-trimethylsilane, as both H₂O and HF scavenger via breaking the active Si–N bond [11]. Zhang reported that the flammability of the alkylcarbonate electrolytes was effectively suppressed with adding 10 vol% vinyl-tri-(methoxydiethoxy) silane [12]; Walkowiak *et al.* declared that the polyether-functionalized disiloxanes could be used as a film forming additive to prevent graphite exfoliation in propylene carbonate based electrolytes [13].

In this paper, we report a novel series of aminoalkylsilane compounds with oligo(ethylene oxide) units as multifunctional electrolyte additives for LIBs. These compounds are designed based on the oligo(ethylene oxide) chain end-capped with organosilicon functional group and alkylamine group on each end. The oligo(ethylene oxide)

*Corresponding author (email: lzzhang@ms.giec.ac.cn)

chain provides the ability to complex lithium ions to ensure the solvation of lithium salts; and the alkylamine group acts as an acid scavenger (HF generated from the decomposition reaction of electrolytic salt) so as to improve the cycleability of the cells [14]. The organosilicon groups, such as trimethylsilyl, disiloxanyl, and triethoxyethyl group, may introduce specific properties to the designed compounds like flame retardant property, passive film forming capability on the electrodes [10–13].

2 Experimental

2.1 Materials and measurements

Allylbromide, *N,N*-dimethyl ethanolamine, 2-[2-(dimethylamino)ethoxy]ethanol, and organosilicon raw materials for the synthesis of electrolyte additives are commercially available and used without further purification. Battery grade materials were used as received: LiPF₆, dimethyl carbonate (DEC), and ethylene carbonate (EC) (H₂O < 20 ppm, Zhangjiagang Guotai-Huarong, China); LiCoO₂ (Hunan Reshine New Material Co.); Li foil (China Energy Lithium); aluminum foil (99.99% purity, 0.5 mm thick, Shenzhen Weifeng DianZi), separator (Celgard 2325).

¹H NMR, ¹³C NMR and ²⁹Si NMR were taken on a Bruker avence 600 spectrophotometer or on a Varian Mercury Vx300. The water contents of the synthesized organosilicon compounds were less than 30 ppm, which were measured by Karl-Fisher coulometric moisture titrator (831 KF). Viscosity (η) measurements were performed on a multi-speed digital viscometer (Shanghai Nirun Intelligent Technology Co., SNB-2). The dielectric constants (ϵ) were measured on an 870 Liquid Dielectric Constant Meter (Scientifica). DSC data were obtained using a NETZSCH DSC204C instrument, calibrated with indium and polydimethylsiloxane. All samples were cooled with liquid nitrogen down to -150 °C, followed by heating from -150 °C to 60 °C at a rate of 10 °C/min. The glass transition temperature (T_g) value was determined from the onset of the glass transition of the second heat run. Ionic conductivities were determined by DDS-310 conductivity instrument, variable temperature conductivity measurements were conducted in a water bath for temperature ranging between 0 °C and 80 °C. EIS results were obtained with a Zennium/IM6 electrochemical workstation (Zahner, Germany) with 5 mV AC amplitude in the frequency range of 0.01 Hz to 100 kHz. X-ray photoelectron spectroscopy (XPS) tests of LiCoO₂ electrodes were performed with ESCALAB 250 (Thermo Fisher Scientific, USA) at 2×10^{-9} mbar. Al K α (1486.6 eV) was used as the X-ray source at 15 Kev of anode voltage. Before XPS test, the cycled LiCoO₂ electrode was washed three times with pure DEC followed by vacuum drying overnight at room temperature. Energy dispersive spectroscopy (EDS) (FE SEM Hitachi S-4800 Japan)

was used to inspect the surface element composition of the electrodes.

2.2 Synthesis of the aminoalkylsilanes

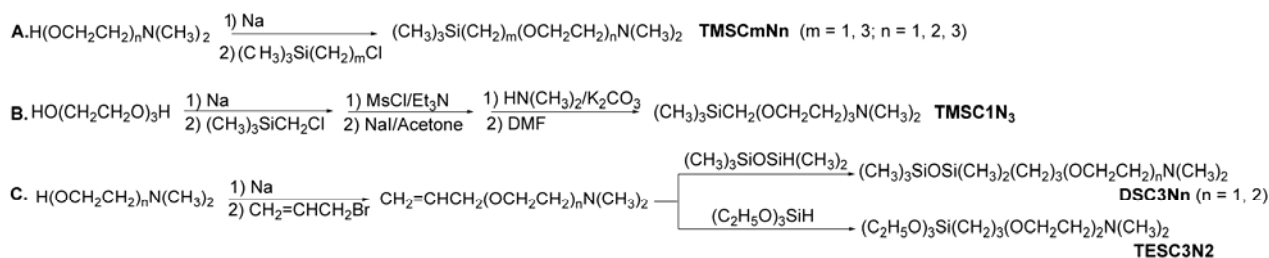
The synthesis of aminoalkylsilane, TMSCmNn (m=1, 3; n=1–3), is shown in Scheme 1. TMSCmNn (m=1, 3; n=1, 2) was synthesized by a nucleophilic substitution reaction of ethanolamine sodium salt with the corresponding chlorosilane. TMSCmNn (m=1; n=3) as an exception example was synthesized in a four-step procedure outlined in route B due to the commercial unavailability of 2-(2-(2-(dimethylamino)ethoxy)ethoxy) ethanol. DSC3Nn (n=1, 2) and TESC3N2 were prepared by an H₂PtCl₆ catalyzed hydrosilylation reaction of allyloxyethoxy substituted dialkylamine with pentamethyldisiloxane and triethoxysilane respectively (route C). All products were purified by repeated distillation and monitored by gas chromatography to ensure >99% purity; their chemical structures were confirmed by NMR.

Typical procedures for the synthesis of DSC3N1: to a two-necked 250 mL flask, 2-(allyloxy)-*N,N*-dimethylethanolamine (10.6 g, 82 mmol), pentamethyldisiloxane (13.9 g, 94 mmol), and H₂PtCl₆ (catalytic amount 0.4% mmol) were added, and the reaction mixtures were stirred at 90 °C until the completion of the reaction. After that, the product was purified by distillation giving colorless liquid with the yield of 85%, b.p.: 47 °C/0.7 mmHg; ¹H NMR (600 MHz, CDCl₃): 3.49–3.52 (t, 2H, -OCH₂CH₂N), 3.36–3.40 (t, 2H, CH₂OCH₂CH₂N), 2.47–2.50 (t, 2H, -CH₂N), 2.26 (s, 6H, -N(CH₃)₂), 1.57–1.61 (m, 2H, -CH₂CH₂Si), 0.46–0.50 (m, 2H, -CH₂CH₂Si), 0.02–0.05 (d, 15H, -Si(CH₃)₂OSi(CH₃)₃); ¹³C NMR (150.9 MHz, CDCl₃): 74.08, 58.92, 45.85, 23.38, 14.26, 1.92, 0.22; ²⁹Si NMR (59.6 MHz, CDCl₃): 8.94, 9.16. DSC3N2 and TESC3N2 were synthesized with the similar procedure of DSC3N1.

DSC3N2: yield: 74%; b.p.: 98 °C/0.2 mmHg; ¹H NMR (600 MHz, CDCl₃): 3.56–3.61 (m, 6H, OCH₂CH₂OCH₂), 3.39–3.42 (t, 2H, OCH₂CH₂CH₂Si), 2.49–2.51 (t, 2H, CH₂N), 2.25 (s, 6H, N(CH₃)₂), 1.57–1.60 (m, 2H, CH₂CH₂Si), 0.46–0.49 (m, 2H, CH₂Si), 0.02–0.04 (d, 15H, Si(CH₃)₃). ¹³C NMR (150.9 MHz, CDCl₃): 74.22, 70.40, 70.02, 69.35, 58.82, 45.85, 23.38, 14.19, 1.93, 0.23. ²⁹Si NMR (59.6 MHz, CDCl₃): 8.82, 9.04.

TESC3N2: yield: 74%; b.p.: 97–98 °C/0.2 mmHg; ¹H NMR (600 MHz, CDCl₃): 3.77–3.78 (m, 6H, (CH₃CH₂O)₃Si), 3.54–3.57 (m, 6H, OCH₂CH₂OCH₂), 3.40 (m, 2H, SiCH₂CH₂CH₂O), 2.47 (m, 2H, OCH₂CH₂N), 2.23 (s, 6H, N(CH₃)₂), 1.66 (m, 2H, SiCH₂CH₂CH₂), 1.17 (m, 9H, Si(OCH₂CH₃)₃), 0.59 (m, 2H, SiCH₂CH₂CH₂). ¹³C NMR (150.9 MHz, CDCl₃): 73.62, 70.39, 69.99, 69.35, 58.82, 58.35, 45.84, 22.92, 18.25, 6.42. ²⁹Si NMR (59.6 MHz, CDCl₃): -43.24.

Typical procedures for the synthesis of TMSC1N1: to a



Scheme 1 Synthetic routes of multifunctional aminoalkylsilanes.

two-necked 250 mL flask, *N,N*-dimethylethanolamine (38 g, 0.42 mol) and sodium (3.6 g, 0.16 mol) were added, and the reaction mixtures were heated until the sodium disappeared completely. After cooling to room temperature, (chloromethyl)trimethylsilane (20.0g, 0.16 mol) was added dropwise, and then the reaction mixtures were stirred vigorously for 48 h at 110 °C. After completion of the reaction, the product was extracted with hexane and separated by distillation elaborately. **TMSC1N1**: yield: 66%, b.p.: 160 °C. ^1H NMR(600MHz, CDCl_3): $\delta = -0.01$ (s, 9H, $\text{Si}(\text{CH}_3)_3$), 2.22 (s, 6H, $\text{N}(\text{CH}_3)_2$), 2.38 (t, $J=6.0$ Hz, 2H, NCH_2), 3.07 (s, 2H, SiCH_2O), 3.45 (t, $J=6.0$ Hz, 2H, $\text{OCH}_2\text{CH}_2\text{OCH}_2$); ^{13}C NMR (150.9 MHz, CDCl_3): 0.00, 49.17, 61.72, 68.30, 77.16; ^{29}Si NMR (119.3 MHz, CDCl_3): $\delta = -2.62$. **TMSC1N2**, **TMSC3N1**, and **TMSC3N2** were synthesized with the similar procedure of **TMSC1N1**.

TMSC1N2: yield: 67%; b.p.: 34–35 °C/0.2 mmHg; ^1H NMR(600 MHz, CDCl_3): $\delta = 0.01$ (s, 9H, $\text{Si}(\text{CH}_3)_3$), 2.24 (s, 6H, $\text{N}(\text{CH}_3)_2$), 2.47 (t, $J=5.8$, 2H, NCH_2), 3.12 (s, 2H, SiCH_2O), 3.55 (m, 6H, $\text{OCH}_2\text{CH}_2\text{OCH}_2$). ^{13}C NMR (150.9 MHz, CDCl_3): $\delta = -2.91$, 46.02, 59.10, 65.53, 69.59, 70.35, 74.92. ^{29}Si NMR (119.3 MHz, CDCl_3): $\delta = -2.99$.

TMSC3N1: yield: 67%; b.p.: 201–203 °C; ^1H NMR(600 MHz, CDCl_3): $\delta = -0.01$ (s, 9H, $\text{Si}(\text{CH}_3)_3$), 0.47 (m, 2H, $(\text{CH}_3)_3\text{SiCH}_2$), 1.60 (m, 2H, $(\text{CH}_3)_3\text{SiCH}_2\text{CH}_2$), 2.28 (s, 6H, $\text{N}(\text{CH}_3)_2$), 2.51 (t, $J=5.7$ Hz, 2H, $\text{CH}_2\text{N}(\text{CH}_3)_2$), 3.47 (t, $J=7.2$ Hz, 2H, $(\text{CH}_3)_3\text{SiCH}_2\text{CH}_2\text{CH}_2$), 3.60 (t, $J=5.7$ Hz, $\text{CH}_2\text{CH}_2\text{N}(\text{CH}_3)_2$); ^{13}C NMR (150.9 MHz, CDCl_3): $\delta = -0.00$, 14.28, 25.77, 47.68, 60.75, 70.59, 75.99; ^{29}Si NMR (119.3 MHz, CDCl_3): 0.52.

TMSC3N2: yield: 72%; b.p.: 53 °C/0.2 mmHg; ^1H NMR(600 MHz, CDCl_3): $\delta = -0.02$ (s, 9H, $\text{Si}(\text{CH}_3)_3$), 0.47 (m, 2H, $(\text{CH}_3)_3\text{SiCH}_2$), 1.58 (m, 2H, $(\text{CH}_3)_3\text{SiCH}_2\text{CH}_2$), 2.27 (s, 6H, $\text{N}(\text{CH}_3)_2$), 2.52 (t, $J=6.0$, 2H, $\text{CH}_2\text{N}(\text{CH}_3)_2$), 3.42 (t, $J=7.2$, 2H, $(\text{CH}_3)_3\text{SiCH}_2\text{CH}_2\text{CH}_2$), 3.61 (m, 6H, $\text{TMSC}_3\text{OCH}_2\text{CH}_2\text{OCH}_2$); ^{13}C NMR (150.9 MHz, CDCl_3): 0.03, 14.24, 25.73, 47.70, 60.59, 71.18, 71.78, 72.18, 76.07; ^{29}Si NMR (119.3 MHz, CDCl_3): 0.49.

TMSC1N3 was synthesized as Scheme 1B: yield: 76%; b.p.: 90 °C/0.5 mmHg; ^1H NMR(600 MHz, CDCl_3): $\delta = 0.10$ (s, 6H, $\text{Si}(\text{CH}_3)_2$), 2.22 (s, 12H, NCH_3), 2.45 (t, 4H, $J=5.8$ Hz, NCH_2CH_2), 3.523 (m, 8H, $\text{SiO}(\text{CH}_2\text{CH}_2\text{O})_2$), 3.79 (t, 4H, $J=5.4$ Hz, NCH_2). ^{13}C NMR (150.9 MHz, CDCl_3): $\delta = -0.00$, 48.99, 61.98, 68.85, 72.56, 75.29. ^{29}Si NMR (119.3 MHz, CDCl_3): $\delta = -1.75$.

2.3 Cells preparation

Working electrodes were prepared by mixing LiCoO_2 , carbon black and polyvinylidene fluoride (PVDF) at a weight ratio of 80:10:10 in *N*-Methyl-2-pyrrolidone (NMP), and then the slurry was spread onto an Al foil and dried at 80 °C under vacuum for 6 h. The lithium metal (99.9%) was used as the counter electrode. All the cells were assembled under a dry argon atmosphere in the glove box (Mikrouna, H_2O and $\text{O}_2 < 1$ ppm). The constant current discharge and charge measurements were carried out with a multi-channel battery test system (NEWARE BTS-610) using coin-type cells (CR2025) at room temperature.

3 Results and discussion

3.1 Basic physical and electrochemical properties

Basic physical and electrochemical properties of the synthesized compounds, such as viscosity (η), dielectric constant (ϵ), glass transition temperature (T_g), and ion conductivity (σ), are summarized in Table 1. Both the dielectric constant and ionic conductivity of these compounds increased with increasing ethylene oxide (EO) chain length, even though the viscosity correspondingly increased at the same time. In addition, the ionic conductivities of these compounds with the same amino ether chain structure were significantly affected by the organosilicon group and methylene spacer length. For instance, the conductivity of trimethyl compounds decreased notably with increasing the carbon spacer length, possibly due to the decreased viscosity. The ionic

Table 1 Physical data, conductivity for the aminoalkylsilanes

Compound	η (cP) ^[a]	ϵ ^[a]	T_g (°C)	σ (mS/cm) ^[a]
TMSC1N1	1.29	2.85	-138	0.50
TMSC1N2	2.30	3.39	-119	0.77
TMSC1N3	2.98	5.40	-106	0.81
TMSC3N1	1.72	3.31	-127	0.44
TMSC3N2	2.70	3.80	-116	0.60
DSC3N1	2.04	2.86	-122	0.33
DSC3N2	3.28	3.21	-112	0.34
TESC3N2	3.52	4.35	-114	0.70

a) Data were corrected at 25 °C, and the conductivity was measured with doping 1M LiTFSI.

conductivity of these aminoalkylsilanes ranges between 0.33 and 0.81 mS/cm at room temperature. Among them, TMSC1N3 with one methylene spacer and three EO units showed the highest ionic conductivity. The Arrhenius plots of the ionic conductivity of the electrolytes were slightly curved (Figure 1(a)), suggesting that the motion of EO chains plays a role in the ionic conductivity of the electrolytes [9(a)]. The differential scanning calorimetry (DSC) curves of these compounds are depicted in Figure 1(b), showing that T_g increased with increasing the chain length of EO units and methylene spacer, and only one second-order phase inflection for T_g at low temperature (<-100 °C). Therefore, the aminoalkylsilanes are suitable for low temperature applications because these compounds are in a completely amorphous state within the low temperature range studied [9(b)].

3.2 Cell tests

Thanks to the acid scavenger function of amino group and interfacial film forming property of disiloxanyl group on LiCoO_2 electrode [15], we picked DSC3N1 to investigate its effect on the cell performance of LiCoO_2 cathode, a most commonly used cathode material in LIBs [16]. Figure 2(a) shows the specific charge/discharge capacities versus cycle number for LiCoO_2/Li cell using 1.0 M LiPF_6 in EC:DEC

(1:1, in volume) as electrolyte with/without 1 vol% DSC3N1 additive, which is an optimized addition volume through parallel experiments. The cell was charged and discharged at the rate of 0.2 C with the cut-off voltage of 3.0–4.2 V vs Li/Li^+ . The discharge capacity of LiCoO_2/Li cell at the 1st and the 100th circle with DSC3N1 addition (compared with that of the base electrolyte) is 135 mAh/g (136 mAh/g) and 113 mAh/g (104 mAh/g), respectively. The LiCoO_2/Li cell with 1 vol% DSC3N1 additive showed better capacity retention (89%) than that of the base electrolyte cell (80%) after 100 cycles, indicating that the cyclic performance of LiCoO_2/Li cell is improved significantly in the electrolyte containing DSC3N1 additive. It has been generally recognized that the acidic impurities in electrolytes originate from two factors: (1) the existence of low content of water and acidic impurities in electrolyte before use, and (2) chemical oxidation of the electrolyte solvents by oxygen released from cathode during occasional overcharging [17]. This improved cycling capability could be attributed to the alkylamine group of DSC3N1 which prevented deteriorating the performance of LiCoO_2 by acidic impurities in the electrolyte [2, 14]. The LiCoO_2/Li cell with DSC3N1 addition also exhibited improved C-rate performance (Figure 2(b)), retaining 86%/65% capacity retention as compared with 65%/1% for the cell without DSC3N1 additive at 1C/5C rate, respectively. When further cycled at

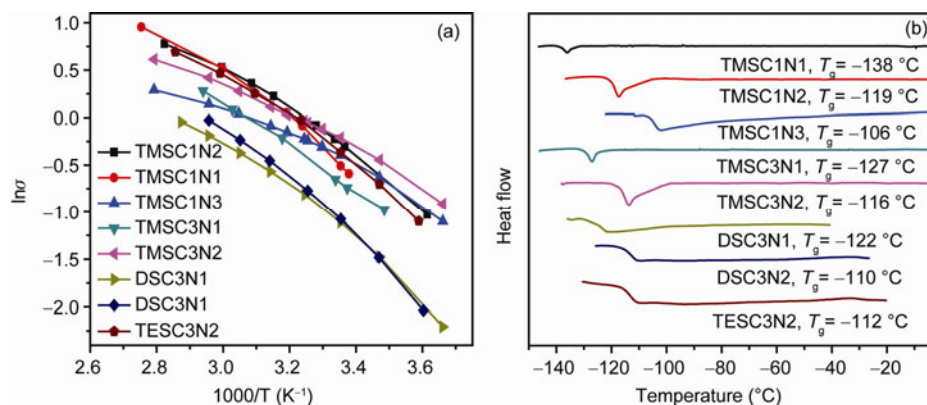


Figure 1 (a) Arrhenius plots of the ionic conductivity of the aminoalkyl silanes with 1M LiTFSI salt; (b) DSC traces of the aminoalkylsilanes.

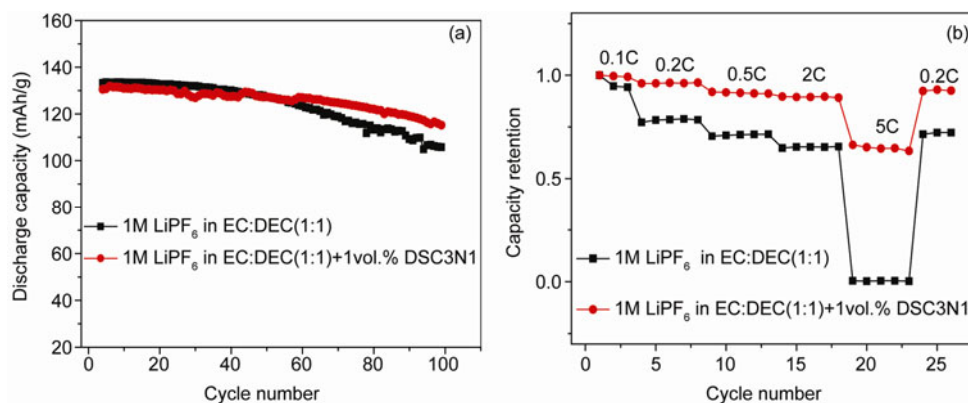


Figure 2 Cycling performances (a) and C-rate performances (b) of LiCoO_2/Li cell in different electrolytes.

0.2C after 5C test, both of the cells with/without DSC3N1 recovered the capacity to the former 0.2C level, indicating that DSC3N1 had a positive function on improving the C-rate performance of LiCoO₂/Li cells. The rate capability of the cells depends on the reaction kinetics of electron transfer and Li⁺ ion transfer to a large extent. Extensive studies have been devoted to improving the electron transfer rate of LiCoO₂ cathode by modifying its particle size, morphology, porosity, and elemental composition [18]. As far as we know, DSC3N1 is one of a few compounds reported so far which improved the rate performance of LiCoO₂ cathode when used as an additive in the electrolytes [19].

3.3 Electrochemical impedance spectroscopy analysis

The electrochemical impedance spectroscopy (EIS) measurements of the cells with/without DSC3N1 additive after 20 cycles and charged to 4.2 V are provided in Figure 3. All the Nyquist plots are composed of two partially overlapping semi-circles at high and medium frequency range and a straight sloping line at the low frequency end, representing respectively three resistance components: film resistance (R_f), charge transfer resistance (R_{ct}), and Li⁺ diffusion resistance [20]. Nyquist plots were fitted with the equivalent circuit shown in the inset of Figure 3. R_e represents the electrolyte resistance and Q_d is the diffusion capacitance attributed by the diffusion process of the Li⁺ in the pore channel of the electrode materials. R_{f1} and R_{f2} correspond to the multilayer surface film resistance and R_{ct} is the charge transfer resistance of Li⁺ at the interface between electrolyte and electrode [19]. Typical parameters are summarized in Table 2, revealing that the R_f (containing R_{f1} and R_{f2}) and R_{ct} for the LiCoO₂ without DSC3N1 additive are 15.8 Ω and 13.3 Ω; whereas for the LiCoO₂ with DSC3N1 additive, they are drastically reduced to 12.1 Ω and 4.3 Ω, respectively, suggesting the enhanced kinetics of Li⁺ transport and hence improved C-rate performance with DSC3N1 additive.

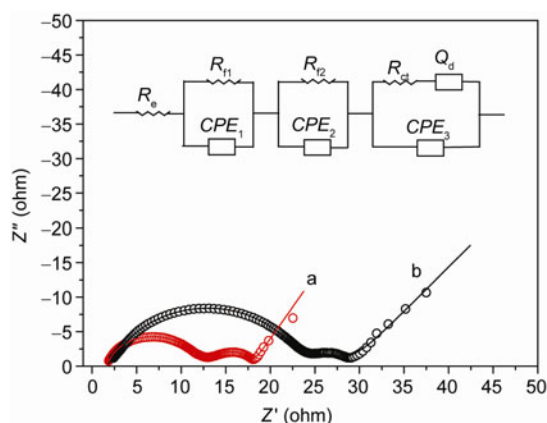


Figure 3 Nyquist plots of LiCoO₂ electrodes with (a) or without (b) DSC3N1 additive. The spots (○) correspond to the experimental data, the solid lines stand for the calculated data from the equivalent circuits (inset).

Table 2 Typical fitting parameters for the Nyquist plots in Figure 3

LiCoO ₂ samples	R_{f1} (Ω)	R_{f2} (Ω)	R_{ct} (Ω)
Without DSC3N1 additive	7.83	7.99	13.33
With DSC3N1 additive	9.36	2.70	4.23

3.4 Surface analysis

The X-ray photoelectron spectroscopy (XPS) of LiCoO₂ electrodes cycled with or without DSC3N1 addition in the electrolyte was conducted to analyze their surface components. Comparing the F1s spectrum of LiCoO₂ electrodes cycled with (Figure 4(a)) and without DSC3N1 addition (Figure 4(b)), we found that the relative content of LiF (according to the integration of LiF peak using PVDF as reference) decreased significantly in the case with DSC3N1 addition. We presume this to the HF acid scavenging function of DSC3N1 containing amine group as shown in reaction (3), which reduced the LiF deposition by suppressing the reaction of LiCoO₂ with HF shown in reaction (2) [21]. Accordingly, R_f and R_{ct} were decreased due to less deposition of high resistance LiF on the surface of LiCoO₂, as seen in Table 2.



On the other hand, Si2p spectrum revealed that Si-containing species (Si–C, Si–O) were observed on the surface films of LiCoO₂ electrode cycled with the addition of DSC3N1 (Figure 4(c)). Energy dispersive spectroscopy (EDS) analysis also confirmed a silicon signal with an element weight of 0.20% at 1.8 keV related to C, O, F, and P atoms on LiCoO₂ electrode of the cell with DSC3N1 additive after 30 cycles (Figure 4(d)). Based on these data, we can conclude that disiloxanyl group in DSC3N1 was apparently involved in the formation of passive film on the surface of LiCoO₂ electrode. Similar to the report of disiloxanyl compound participating in passive film formation on the surface of LiCoO₂ [15], the passive film formation property of DSC3N1 is likely to suppress the LiF formation on LiCoO₂ electrode thus reduced the impedance of LiCoO₂ electrode and improved the C-rate performance of LiCoO₂/Li cell shown in Figure 2(b).

4 Conclusions

In conclusion, we reported a new series of aminoalkylsilane compounds with oligo(ethylene oxide) units as multifunctional electrolyte additives for LIBs. These compounds have low viscosities, high conductivities, and very low glass transition temperatures. The LiCoO₂/Li cell exhibited improved cyclability and rate performance with adding 1 vol%

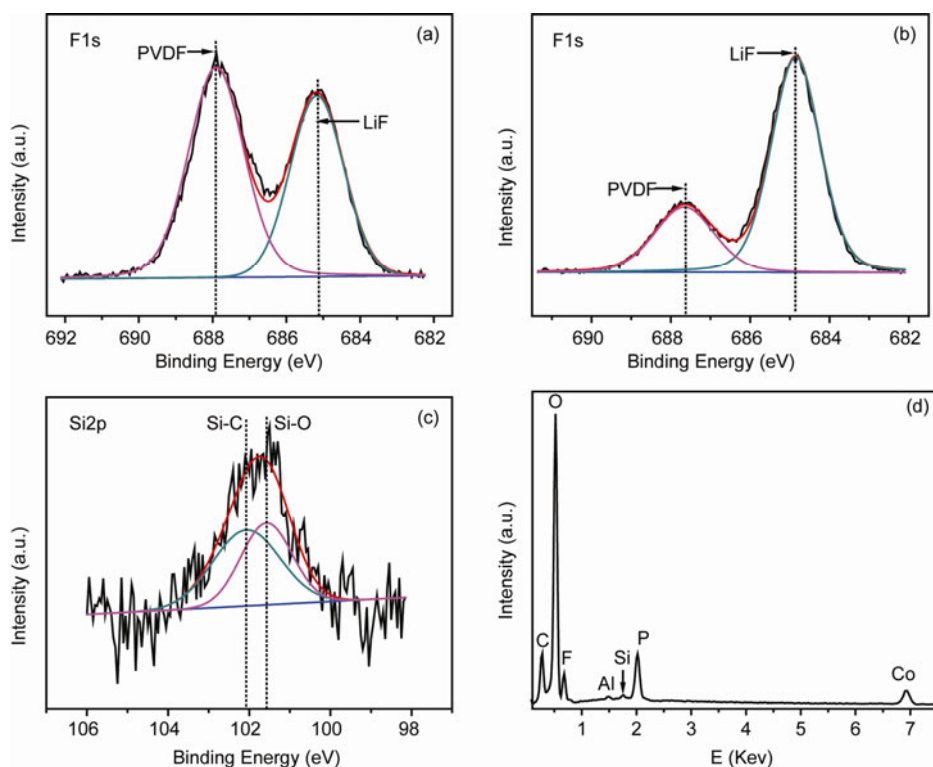


Figure 4 XPS spectrum of F1s detected on the LiCoO₂ electrode cycled (a) with/(b) without DSC3N1 addition; (c) XPS spectrum of Si2p detected on the LiCoO₂ electrode cycled with DSC3N1; (d) EDS of LiCoO₂ electrode after 30 cycles for the cell with DSC3N1 addition.

DSC3N1 in the base electrolyte. EIS, XPS, and EDS experiments revealed that the interfacial impedance of the cell and the relative content of LiF on the surface of LiCoO₂ were decreased significantly with DSC3N1 additive in the base electrolyte, due to the acid scavenging and passive film forming function of DSC3N1. These results demonstrate that these aminoalkylsilanes have considerable potential as electrolyte additives for use in lithium-ion batteries.

This work was supported by the National Natural Science Foundation of China (50973112), the Hundred Talents Program of Chinese Academy of Sciences (CAS), CAS-Guangdong Collaboration Program (20108), and Guangzhou Municipal Science & Technology Project (11A44061500).

- 1 a) Etacheri V, Marom R, Elazari R, Salitra G, Aurbach D. Challenges in the development of advanced li-ion batteries: A review. *Energy Environ Sci*, 2011, 4: 3243-3262; b) Xu K, Nonaqueous liquid electrolytes for lithium-based rechargeable batteries. *Chem Rev*, 2004, 104: 4303-4417
- 2 Zhang SS. A review on electrolyte additives for lithium-ion batteries. *J Power Sources*, 2011, 162: 1379-1394
- 3 Shim EG, Nam TH, Kim HS, Moon SI. Effects of functional electrolyte additives for Li-ion batteries. *J Power Sources*, 2007, 172: 901-907
- 4 Wang X, Yasukawa E, Kasuya S. Nonflammable trimethyl phosphate solvent-containing electrolytes for lithium-ion batteries: I. Fundamental properties. *J Electrochem Soc*, 2001, 148: A1058-A1065
- 5 Xu MQ, Zhou L, Hao LS, Xing LD, Li WS, Lucht BT. Investigation and application of lithium difluoro(oxalate)borate (LiDFOB) as additive to improve the thermal stability of electrolyte for lithium-ion batteries. *J Power Sources*, 2011, 196: 6794-6801
- 6 Moshurchak LM, Buhrmester C, Wang RL, Dahn JR. Comparative studies of three redox shuttle molecule classes for overcharge protection of LiFePO₄-based Li-ion cells. *Electrochim Acta*, 2007, 52: 3779-3784
- 7 Yang L, Lucht BL. Inhibition of electrolyte oxidation in lithium ion batteries with electrolyte additives. *Electrochem Solid State Lett*, 2009, 12: A229-A231
- 8 a) Rossib NAA, West R. Silicon-containing liquid polymer electrolytes for application in lithium ion batteries. *Polym Int*, 2009, 58: 267-277; b) Tse KY, Zhang LZ, Baker SE, Nichols BM, West R, Hamers RJ. Vertically aligned carbon nanofibers coupled with organosilicon electrolytes: Electrical properties of a high-stability nanostructured electrochemical interface. *Chem Mater*, 2007, 19: 5734-5741; c) Weng W, Zhang ZC, Lu J, Amine K. A disiloxane-functionalized phosphonium-based ionic liquid as electrolyte for lithium-ion batteries. *Chem Commun*, 2011, 47: 11969-11971
- 9 a) Zhang LZ, Zhang ZC, Harring S, Straughan M, Butorac M, Chen ZH, Lyons LJ, Amine K, West R. Highly conductive trimethylsilyl oligo(ethylene oxide) electrolytes for energy storage applications. *J Mater Chem*, 2008, 18: 3713-3717; b) Zhang LZ, Lyons L, Newhouse J, Zhang ZC, Straughan M, Chen ZH, Amine K, Hamers RJ, West R. Synthesis and characterization of alkylsilane ethers with oligo(ethylene oxide) substituents for safe electrolytes in lithium-ion batteries. *J Mater Chem*, 2010, 20: 8224-8226; c) Amine K, Wang QZ, Vissersa DR, Zhang ZC, Rossib NAA, West R. Novel silane compounds as electrolyte solvents for Li-ion batteries. *Electrochem Commun*, 2006, 8: 429-433
- 10 Xia Q, Wang B, Wu YP, Luo HJ, van Ree T. Phenyl tris-2-methoxydiethoxy silane as an additive to PC-based electrolytes for lithium-ion batteries. *J Power Sources*, 2008, 180: 602-606
- 11 Takechi K, Shiga T. Nonaqueous electrolytic solution for battery and nonaqueous electrolytic solution battery. US Patent 6235431, 2001
- 12 Zhang HP, Xia Q, Wang B, Yang LC, Wu YP, Sun DL, Gan CL, Luo

- HJ, Bebeda AW, van Ree T. Vinyl-Tris-(methoxydiethoxy)silane as an effective and ecofriendly flame retardant for electrolytes in lithium ion batteries. *Electrochem Commun*, 2009, 11: 526–529
- 13 Walkowiak M, Waszak D, Schroeder G, Gierczyk B. Polyether-functionalized disiloxanes as new film-forming electrolyte additive for Li-ion cells with graphitic anodes. *Electrochem Commun*, 2008, 10: 1676–1679
- 14 Takechi K, Koiwai A. Nonaqueous electrolytic solution for battery and nonaqueous electrolytic solution battery. US Patent 6077628, 2000
- 15 Markovsky B, Nimberger A, Talyosef Y, Rodkin A, Belostotskii AM, Salitra G, Aurbach D, Kim HJ. On the influence of additives in electrolyte solutions on the electrochemical behavior of carbon/LiCoO₂ cells at elevated temperatures. *J Power Sources*, 2004, 136: 296–302
- 16 Takeuchi T, Kyuna T, Morimoto H, Tobishima S. Influence of surface modification of LiCoO₂ by organic compounds on electrochemical and thermal properties of Li/LiCoO₂ rechargeable cells. *J Power Sources*, 2011, 196: 2790–2801
- 17 Wang E, Ofer D, Bowden W, Ilchev N, Moses R, Brandt K. Stability of lithium ion spinel cells. III. Improved life of charged cells. *J Electrochem Soc*, 2000, 147: 4023–4028
- 18 Zhao Y, Xia D, Li Y, Yu C. Investigation of High-rate spherical LiCoO₂ with mesoporous structure via self-assembly in microemulsion. *Electrochem Solid State Lett*, 2008, 11: A30–A33, and references therein
- 19 Baek B, Jung C. Enhancement of the Li⁺ ion transfer reaction at the LiCoO₂ interface by 1,3,5-trifluorobenzene. *Electrochim Acta*, 2010, 55: 3307–3311
- 20 Zhuang QC, Xu JM, Fan XY, Dong QF, Jiang YX, Huang L, Sun SG. An electrochemical impedance spectroscopic study of the electronic and ionic transport properties of LiCoO₂ cathode. *Chin Sci Bull*, 2007, 52: 1187–1195
- 21 Takanashi Y, Orikasa Y, Mogi M, Oishi M, Murayama H, Sato K, Yamashige H, Takamatsu D, Fujimoto T, Tanida H, Arai H, Ohta T, Matsubara E, Uchimoto Y, Ogumi Z. Thickness estimation of interface films formed on Li_{1-x}CoO₂ electrodes by hard X-ray photoelectron spectroscopy. *J Power Sources*, 2011, 196: 10679–10685